FULL PAPERS

Magnetic Resonance in Medicine 55:271–278 (2006)

Sensitivity-Enhanced ^{13}C MR Spectroscopy of the Human Brain at 3 Tesla

D.W.J. Klomp,[1*] W.K.J. Renema,[1] M. van der Graaf,[1] B.E. de Galan,[2] A.P.M. Kentgens,[3] and A. Heerschap[1]

A new coil design for sensitivity-enhanced ^{13}C MR spectroscopy (MRS) of the human brain is presented. The design includes a quadrature transmit/receive head coil optimized for ^{13}C MR sensitivity. Loss-less blocking circuits inside the coil conductors allow this coil to be used inside a homogeneous circularly polarized ^{1}H B_1 field for ^{1}H decoupled ^{13}C MRS. A quadrature ^{1}H birdcage coil optimized for minimal local RF heating makes broadband ^{1}H decoupling in the entire human brain possible at 3 Tesla while remaining well within international safety guidelines for RF absorption. Apart from a substantial increase in sensitivity compared to conventional small linear coils, the quadrature ^{13}C coil combined with the quadrature ^{1}H birdcage coil allows efficient cross polarization (CP) in the brain, resulting in an additional 3.5-fold sensitivity improvement compared to direct ^{13}C measurements without nuclear Overhauser enhancement (NOE) or polarization transfer. Combined with the gain in power efficiency, this setup allows broadband ^{1}H to ^{13}C CP over large areas of the brain. Clear ^{13}C resonances from glutamate (Glu), glutamine (Gln), aspartate (Asp), lactate (Lac), and γ-aminobutyrate (GABA) carbon spins in the human brain demonstrate the quality of ^{13}C MR spectra obtained in vivo with this coil setup. Magn Reson Med 55: 271–278, 2006. © 2005 Wiley-Liss, Inc.

Key words: ^{13}C MRS; RF coil; cross polarization; SAR; glucose metabolism

In vivo ^{13}C magnetic resonance spectroscopy (MRS) is a powerful tool for continuous, noninvasive monitoring of tissue concentrations of metabolites and metabolic fluxes in humans and animals. For instance, ^{13}C MRS combined with the administration of ^{13}C-enriched glucose provides a unique window into cerebral carbohydrate metabolism. The incorporation of ^{13}C labeled carbons into amino acids, such as glutamate (Glu), aspartate (Asp), and γ-aminobutyrate (GABA), can be measured to obtain information on the Krebs cycle rate and oxidative metabolism (1,2). More recently, Ross et al. (3) reviewed the potential of ^{13}C MRS for clinical use and showed that it has unique capabilities for monitoring a host of diseases.

Compared to ^{1}H MRS, in vivo ^{13}C MRS has limited sensitivity due to the low gyromagnetic ratio (10.5 MHz/T) and low natural abundance (1.1%) of ^{13}C. Additionally, MR signals of ^{13}C spins are split up due to J-coupling with protons, which reduces sensitivity and spectral resolution. The quality of in vivo ^{13}C MRS can be improved by increasing the B_0 field strength and applying ^{1}H decoupling to suppress the effect of H-C J-coupling. Since the protons of the metabolites of interest have chemical shifts distributed over about 5 ppm, broadband ^{1}H decoupling is essential. Particularly at high field strengths, broadband decoupling requires high RF power, which may cause tissue heating.

Thus at high field strengths, RF coils must be designed for both optimal sensitivity and minimal power deposition. The latter, which is expressed as the specific absorption rate (SAR), should be kept within specified safety values (4,5). Adriany and Gruetter (6) proposed a coil design that uses circularly polarized ^{1}H-decoupling fields rather than linearly polarized fields, and enables broadband ^{1}H decoupling in the human brain at high field within SAR guidelines. This design is a substantial improvement over conventional butterfly coils for ^{1}H decoupling. However, within the sensitive field of surface coils, the local SAR will vary greatly and may exceed safety guidelines (7). Since the B_1 field of the two slightly overlapping ^{1}H surface coils decays linearly with respect to distance (8), the use of ^{1}H decoupling is limited to a small region of the brain in order to stay within local SAR guidelines. Recently it was shown that volume coils with homogeneous B_1 fields have lower local SAR values than quadrature surface coils (7). Therefore, it would be more efficient to use volume coils for ^{1}H decoupling rather than surface coils. In addition, the ^{13}C coil design described by Adriany and Gruetter (6) has not been optimized for best sensitivity. Their ^{13}C coil is linearly polarized due to its restrictive mechanics because mutually inductive couplings have to be minimized. Coil designs that are independent of mutual inductive couplings use coils that are double-tuned for two nuclei. These coils have blocking circuits inside the main conductors and thus avoid interference effects from the two fields. Although many designs for double-tuned coils have been proposed, the signal losses in the blocking circuits are substantial (8). Most of these designs are meant to operate at low field strengths or

[1]Department of Radiology, Radboud University Nijmegen Medical Center, Nijmegen, The Netherlands.

[2]Department of General Internal Medicine, Radboud University Nijmegen Medical Center, Nijmegen, The Netherlands.

[3]Department of Physical Chemistry, Radboud University Nijmegen, Nijmegen, The Netherlands.

Grant sponsors: Dutch Organization for Scientific Research (NWO-ALW); Dutch Diabetes Fund.

*Correspondence to: Dennis W.J. Klomp, Radboud University Nijmegen Medical Center, Department of Radiology (430), P.O. Box 9101, 6500 HB Nijmegen, The Netherlands. E-mail: d.klomp@rad.umcn.nl

Presented in part at the 11th Annual Meeting of ISMRM, Toronto, Canada, 2003, and the 21st Meeting of the European Society for Magnetic Resonance in Medicine and Biology, Copenhagen, Denmark, 2004.

Received 1 February 2005; revised 2 August 2005; accepted 31 August 2005.
DOI 10.1002/mrm.20745
Published online 21 December 2005 in Wiley InterScience (www.interscience.wiley.com).

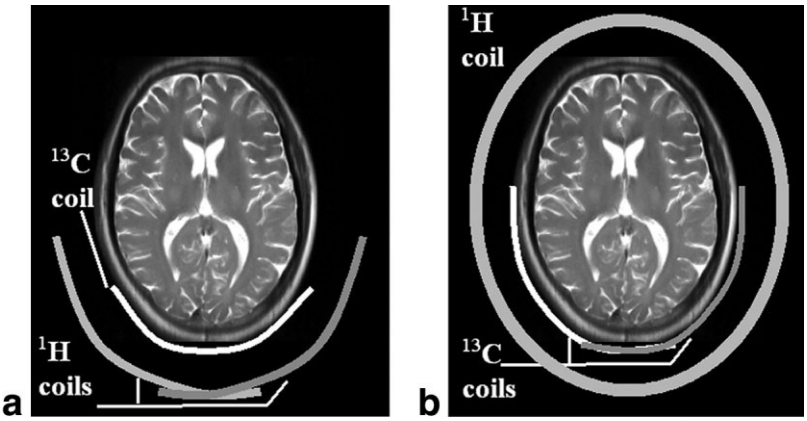

FIG. 1. **a:** The coil concept proposed by Adriany and Gruetter (6) consists of a circularly polarized ^{1}H surface coil with a linearly polarized ^{13}C coil. **b:** Transverse overview of the new coil concept using a birdcage ^{1}H volume coil with a circularly polarized ^{13}C coil positioned close to the human head.

have small coil sizes, which make the coil losses dominant. When large coil sizes are used at high field strengths, the tissue losses become dominant, which makes the effect of additional circuits negligible (8).

Another way to improve ^{13}C MR sensitivity is to transfer ^{1}H magnetization from the ^{1}H spins to the ^{13}C nuclei through cross relaxation or mediated by J-coupling. Using cross relaxation by means of nuclear Overhauser enhancement (NOE), the sensitivity can be changed ranging from a complete signal cancellation up to a threefold $(1+\gamma^{1}H/2\gamma^{13}C)$ enhancement, depending on the molecular structure and environment. Up to a fourfold gain $(\gamma^{1}H/\gamma^{13}C)$ can be accomplished using pulsed polarization transfer methods, such as distortionless enhancement of polarization transfer (DEPT) (9), or cross polarization (CP) (10). While the efficiency of DEPT depends on accurate pulse angles, the efficiency of CP depends on the fulfillment of the Hartman-Hahn condition (i.e., matching of the ^{13}C and ^{1}H B_1 fields). Although CP has only been used in vivo at small bandwidths using WALTZ4 pulse trains (11,12), recent developments in high-resolution NMR have shown that broadband CP using optimized pulse trains is possible (13).

In this paper we introduce a new coil design that substantially improves the sensitivity of ^{13}C MRS at 3 T. First, a homogeneous volume coil is used for efficient ^{1}H decoupling, which leads to minimized local RF absorption. Second, within this volume coil a circularly polarized ^{13}C coil is fitted that is suitably sized to perform sensitive ^{13}C MRS on most of the brain. Moreover, exploiting the favorable properties of this design, we implemented a sequence for ^{1}H–^{13}C CP with broadband ^{1}H decoupling, which allows substantial sensitivity enhancement of ^{13}C MRS over large volumes of the human brain with a broad spectral bandwidth.

MATERIALS AND METHODS

A shielded 16-leg birdcage coil was built with a homogeneous B_1 field for ^{1}H MRI and decoupling in the human head (inner diameter = 25 cm; length = 18 cm). The coil is driven in quadrature mode to obtain a circularly polarized magnetic field. Two slightly overlapping, anatomically shaped ^{13}C coils (diameter = 14 cm) were constructed that can be shifted inside the birdcage coil (Fig. 1a). Since the coupling of the ^{1}H coil with the ^{13}C coils is very high, ^{1}H-blocking circuits inside the ^{13}C coil conductors were incorporated to prevent cross-talk and thus maintain ^{1}H field homogeneity. The circuits consist of a 33pF capacitance parallel to a solenoid coil (four windings, diameter of 6 mm) positioned at 2 cm from the head. The ^{13}C coils were matched to 50 ohm at 31 MHz and connected via a quadrature hybrid box to an in-house-built transmit-receive switch (−0.2 dB), low-pass filter (−0.2 dB at 31 MHz, and −100 dB at 123 MHz), and preamplifier (noise figure = 0.5dB; Advanced Receiver Research, Burlington, USA). The correct construction of the ^{13}C receiver chain is crucial for realizing low-noise ^{13}C signal detection while simultaneously transmitting high RF power for ^{1}H decoupling. Cross-talk can influence the quality of the receiver, particularly if large RF coils at high power are used. Therefore, the low-pass filter is integrated into the preamplifier to prevent saturation. The coils were interfaced to a clinical 3T MR system (Trio; Siemens, Erlangen, Germany) equipped with an additional RF channel (MR Research Systems, Guildford, UK). All MR examinations were performed with the approval of the local ethics committee.

The losses of the ^{1}H blocking circuit were determined by measuring the difference in the quality factor (Q) of the coil with and without the blocking circuit, loaded with a human head (8). For a more accurate determination of the

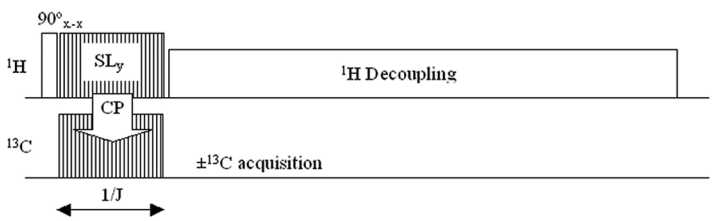

FIG. 2. Pulse sequence used for ^{1}H–^{13}C CP. A spin-locking field (SL_y) is applied directly after excitation of the ^{1}H spins. Simultaneously a ^{13}C B_1 field is applied during an optimal period of 1/J for CP, followed by ^{13}C MR acquisition with ^{1}H decoupling. An 180° phase cycle is used to suppress contributions from direct ^{13}C excitation.

Table 1
Measured Quality Factor Values for the ^{13}C coil, Both Unloaded and Loaded with a Human Head; Upper Row Without a Blocking Circuit, Lower Row with a Blocking Circuit

Block	Q unloaded	Q loaded	Q in ^{1}H coil
No	330	72	N/A
Yes	280	70	70

losses, *Q*-factors were also measured for the unloaded coil. The *Q*-factors of a single coil element were measured using a network analyzer (HP8752A, Hewlett Packard), with the head of a 25-year-old healthy male volunteer as the loading. The performance of the blocking circuit was tested by carefully checking the homogeneity of the ^{1}H field in the head near the conductors of the ^{13}C coil using a spin-echo sequence. An 810° (9 × 90°) excitation pulse was used instead of a 90° pulse to amplify RF inhomogeneities (an 11% (90/810) local difference in excitation angle will result in dark image intensities). The experiment was repeated without the ^{13}C coil.

The overall SNR of the circularly polarized ^{13}C coil including its blocking circuits was compared with an equally sized linearly polarized ^{13}C coil (^{13}C coil diameter = 14 cm; ^{1}H coil diameter = 18 cm; Fig. 1a). To minimize volume effects, the gain in SNR was determined using a small phantom. A 2-ml spherical phantom containing 30% ^{13}C-1-glucose (20% w/w solution) was positioned at 6 cm from the coils and inserted into a large spherical phantom containing 2 L of saline (0.9% NaCl) such that the loading conditions of the ^{13}C coils (*Q*-factor) were identical to those of the in vivo situation. A pulse-acquire sequence with WALTZ16 ^{1}H decoupling was used for both coil setups.

The power efficiency of the ^{1}H birdcage coil was compared with the power efficiency of the coil configuration described by Adriany and Gruetter (6) (Fig. 1a). The B_1 fields per unit of RF power were measured in vivo by using multi-angle gradient-echo sequences in both coils. In addition, temperature maps were measured on a Perspex phantom filled with an agarose gel that contained 1.33 g/l NaCl and 0.66 g/l $CuSO_4$ (14). Both 3D (at low spatial resolution: TE = 34 ms, TR = 910 ms, FOV = 160 × 200 × 200, 8 × 10 × 10 phase encodings, elliptical sampling, 1024 data points at 1250 Hz bandwidth) and 2D (TE = 34 ms, TR = 910 ms, FOV = 160 × 200, 16 × 20 phase encodings, elliptical sampling, 1024 data points at 1250 Hz bandwidth) spectroscopic imaging sequences, with an additional RF heating pulse, were used to image the shift in ^{1}H resonance of water before and after 20 min of RF heating at 3 W/kg. The selected slice for the 2D sequence was positioned at the location of highest temperature rise, measured with the 3D sequence. Eddy current correction was performed for the data, with the measurement before RF heating taken as a reference (15). The time domain data from each voxel were fitted to a monoexponential decay function, and the frequency was used as an absolute measure for temperature change (16). The ratio between local and average temperature increases was used to estimate the local SAR.

The overall efficiency of the coil setup was demonstrated by ^{13}C MRS of the human brain with broadband ^{1}H decoupling. The subjects studied were all nondiabetic, healthy volunteers. A hyperinsulinemic euglycemic glucose clamp was used to achieve euglycemic conditions, as described previously (17). Briefly, insulin was infused at a rate of 60 mU · m^{-2} · min^{-1}, and a variable infusion of isotopically enriched 20% glucose solution was adjusted so that constant plasma glucose levels could be maintained at 5.3±0.1 mmol/L with a coefficient of variation (CV) of 6.1% throughout the experiment. Arterial blood was drawn at 5-min intervals for immediate measurement of plasma glucose levels in duplicate by the glucose oxidation method (Beckmann Glucose Analyzer II; Beckman, Fullerton, CA, USA), and for measurement of plasma isotopic enrichment by high-resolution ^{1}H NMR at 500 MHz. At the start of the clamp, 30 ml of 100% $^{13}C_1$-enriched glucose 20% was infused in 10 min, whereas 30% $^{13}C_1$-enriched glucose 20% was used for the remainder of the clamp. Thus, stable levels of plasma isotopic enrichment (averaging 29.4% ± 1.4%) were obtained within 30 min. Prior to the clamp, 12 ^{13}C MR spectra of 2.5 min each were acquired for a baseline data set (200 μs rectangular excitation pulse, TR = 2 s, 135 ms WALTZ16 ^{1}H decoupling

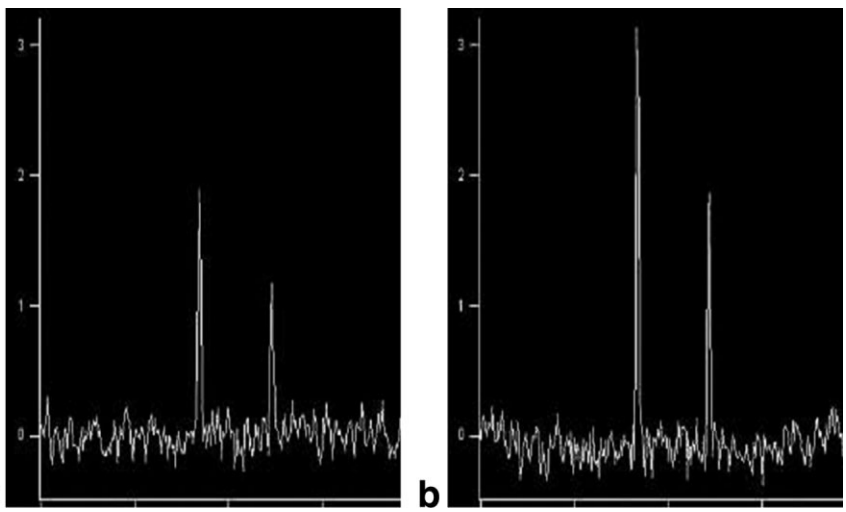

FIG. 3. Improving ^{13}C MRS with a circularly polarized coil. Two ^{1}H-decoupled ^{13}C MR spectra are shown that were acquired from a 2-ml spherical phantom of 30% ^{13}C-1 labeled glucose (20% w/w solution), positioned 6 cm from the coils: (**a**) with the linearly polarized ^{13}C coil, and (**b**) with the circularly polarized ^{13}C coil. The overall gain in SNR realized with circularly polarized ^{13}C coil including the blocking circuits compared to the linearly polarized ^{13}C coil is 40%.

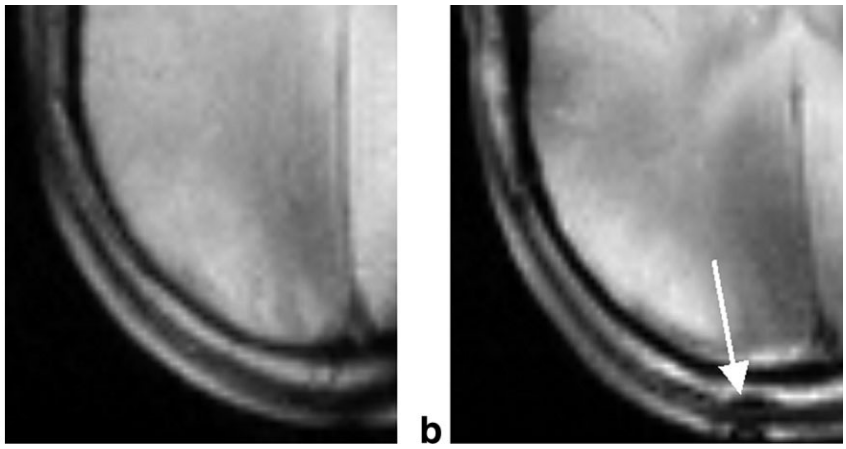

FIG. 4. Spin-echo images acquired with the ^{1}H birdcage coil without (**a**) and with (**b**) the ^{13}C coils inserted. The excitation pulse was set to a 810° flip angle rather than 90° to emphasize B_1 inhomogeneities (as shown by a small black circle, meaning an 11% variation in the RF field strength, at a distance of 8 mm from the ^{13}C coil conductor, indicated by an arrow).

with 700 μs segments). After stable clamp conditions were obtained, another 12 ^{13}C MR spectra of 2.5 min each were acquired under euglycemic conditions. After automatic frequency and phase correction (18) was performed, the 12 ^{13}C MR spectra were averaged and subtracted from the 12 averaged ^{13}C MR baseline spectra.

To explore the possibilities of ^{1}H–^{13}C CP over large volumes with this setup, the signal gain acquired by CP was measured in a phantom and in vivo. A pulse sequence was used with the spin-locking ^{1}H B_1 field and the cross-polarizing ^{13}C B_1 field realized by a WALTZ4 train with a duration of 6.7 ms (i.e., 1/J, using the average coupling of C-H groups in most MR-visible metabolites) (Fig. 2). The ^{13}C MR signals of myo-inositol (at 72.1, 73.3+73.6, and 75.3 ppm) were used as in vivo markers to quantify the efficiency of CP in the human brain.

In general for in vivo measurements, the available bandwidth for CP is low. However, since the coil is more efficient in terms of SAR, the power during the CP can be increased, which increases its bandwidth. Additional increments in bandwidth can be realized using more efficient pulse trains than WALTZ4. Although many pulse trains have been proposed for high-resolution NMR with substantially increased bandwidths, most of these trains are too long to fit into the optimum duration of 6.7 ms for in vivo applications (13). At equal powers, the R_4 pulse train is 4/3 times longer than WALTZ4, but realizes a more than twofold increase in bandwidth (data not shown). Replacing WALTZ4 with an R_4 pulse train and increasing its amplitude 4/3 times such that it fits the optimal duration of 6.7 ms increases the bandwidth to 40 ppm at 3T. The bandwidth of this CP experiment was validated in phantom measurements and in vivo.

RESULTS

Measurements of the *Q*-factor of the new ^{13}C coil unloaded and loaded with the human head clearly showed that the effect of the blocking circuit on the *Q* in the loaded condition is negligible (Table 1). The sensitivity reduction of the ^{13}C coils by the blocking circuits was 2%, i.e.,

$$1 - \sqrt{1 - 70\left(\frac{1}{280} - \frac{1}{330}\right)} \qquad [1]$$

The overall gain in SNR with the circularly polarized ^{13}C coil including the blocking circuits compared to the linearly polarized ^{13}C coil was 40% (Fig. 3).

The local ^{13}C coils had a negligible effect on the field homogeneity of the ^{1}H coil, as is obvious from the undisturbed spin-echo MR images (Fig. 1a and b). To take a closer look at the homogeneity of the ^{1}H field near the ^{13}C coil conductors, we acquired spin-echo images with an excitation pulse angle of 810° (9 × 90°) (Fig. 4). In the image obtained by the ^{1}H coil with the ^{13}C coil inserted (Fig. 4b), a small black circle was observed. We conclude that the excitation pulse locally acts effectively as a 0° or 180° pulse. Therefore, a local inhomogeneity of only 90/810 = 11% is observed at a distance of 8 mm from the conductor of the fully coupled ^{13}C coil.

B_1-field profiles at the proton frequency of the coil configurations (i.e., surface coil or volume coil (Fig. 1a and b)) were measured in the head of a 25-year-old healthy volunteer with the use of a multi-angle gradient-echo sequence. At a distance of 7.5 cm inside the brain (i.e., the radius of the ^{13}C coil), the B_1 field strengths were equal using the same amount of power, while the B_1 field strength at the surface of the head was three times lower for the birdcage coil compared to the surface coil (Fig. 5). According to Faraday's law, a homogeneous RF coil might suggest equally distributed RF heating; however, local SAR can be higher due to the applied electric fields and dielectric resonances (7). Temperature maps of a phantom using the birdcage coil showed that this was indeed the case (Fig. 6). The ratio between the maximum local and global temperature increases, averaged per 1 g or per 10 g of tissue, equaled 2.2 and 1.8, respectively. Since we were working with a global SAR of <3 W/kg, this means that we remained well within the FDA and IEC guidelines of 8 W/kg (4) and 10 W/kg (5), respectively, when the local SAR is taken into account.

To demonstrate that broadband ^{1}H decoupling with the volume coil is possible in vivo, we acquired ^{13}C MR spectra of the human brain, with the circularly polarized ^{13}C coil, during ^{13}C-1-glucose infusion. A WALTZ16 sequence was used for ^{1}H decoupling with a bandwidth of 570 Hz (i.e., 0.9–5.4 ppm at 3 T). The global SAR was 1.2 W/kg (i.e., 70 W * 135 ms/2000 ms/4 kg), assuming that the mass of the head inside the sensitive field of the volume coil was

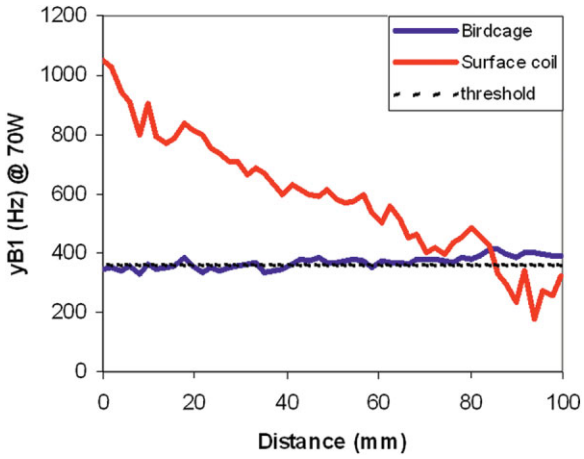

FIG. 5. Profile of the B_1 field in the human brain of the ^{1}H birdcage coil and ^{1}H surface coil. The dashed line indicates the minimum B_1 required for WALTZ16 ^{1}H decoupling at a bandwidth of 570 Hz. Note that the same amount of power is required for both coil setups in order to decouple up to a depth of about 75 mm.

4 kg. Difference spectra obtained from spectra recorded before and during infusion revealed that well-decoupled ^{13}C signals can be obtained with this setup (Fig. 7). Resolved resonances of ^{13}C spins were detected from Glu-C2, Glu-C3, Glu-C4, glutamine (Gln)-C2, Gln-C3, Gln-C4, Asp-C2, Asp-C3, GABA-C2, GABA-C4, lactate (Lac)-C3, α-glucose-C1, and β-glucose-C1.

With the proposed coil design, favorable conditions for sensitivity enhancement by CP can also be realized. The theoretically maximum factor of 4 signal enhancement was measured in a small (50 ml) spherical phantom with ^{13}C-1-glucose, indicating proper sequence conditions. The successful application of WALTZ4-based CP to the human brain was demonstrated by the 3.5-fold sensitivity enhancement of the ^{13}C MR signals of myo-inositol, indicating a good Hartman-Hahn match in the FOV of the ^{13}C coil in the brain (Fig. 8). Although in vivo CP is generally confined to small bandwidths, the replacement of the WALTZ4 by an R_4 pulse increased the bandwidth to approximately 40 ppm at 3 T, as measured in a 50-ml spherical phantom with ^{13}C-1-glucose (Fig. 9). This bandwidth is sufficient for studies applying glucose labeled with ^{13}C at the C-1 position, since most signals of metabolites of interest will appear in the range of 17–57 ppm.

To detect the glucose C-1 MR signals (which resonate at 93 and 97 ppm) as well, an interleaved acquisition can be used to acquire the data in the same time frame. To achieve this, a WALTZ4 CP method with its ^{13}C carrier set to 95 ppm was used interleaved with an R_4 CP method set to 37 ppm for in vivo measurements after ^{13}C-1 glucose infusion. Broadband ^{1}H WALTZ16 decoupling with 700 μs segments for 135 ms was used in both methods at a TR of 2 s. Figure 10a and b show the results of such an interleaved in vivo measurement of the human brain after glucose infusion. With this interleaved method, the bandwidth is effectively increased to about 60 ppm in the same measurement time. SNR is decreased by the square root of 2, but is still substantially higher (more than twofold) compared to that obtained by a direct ^{13}C measurement without NOE or polarization transfer (Fig. 10d). Although additional temperature measurements showed that CP contributed to about 50% of the SAR, all experiments were performed within FDA and IEC guidelines.

DISCUSSION

In this study we have demonstrated that volume-optimized ^{13}C coils can be used in combination with a homogeneous ^{1}H volume coil for broadband ^{1}H decoupled ^{13}C MRS of the human brain at 3 T. The use of circularly polarized coils rather than linearly polarized coils substantially enhances the sensitivity of ^{13}C signal detection. Moreover, with this coil setup we achieved efficient ^{1}H to ^{13}C CP over a large volume in the human brain. A comparison of a conventional surface coil with the volume coil revealed that the maximum local SAR during ^{1}H decoupling was substantially reduced. This enables broadband ^{1}H decoupling and ^{1}H to ^{13}C CP at 3 T within SAR guidelines for either the entire human brain or a selected voxel in the brain using appropriate localization techniques.

Since tissue losses become dominant at high B_0 field strengths (8), additional circuits inserted into the coil become loss-less. This is especially true for large coils, which are positioned close to the tissue. Therefore, the losses of the ^{1}H blocking circuits are negligible and the full benefit of circular polarization can be realized. Once these blocking circuits are inserted into the coils, each coil can be optimized without mechanical restrictions to minimize mutual inductance.

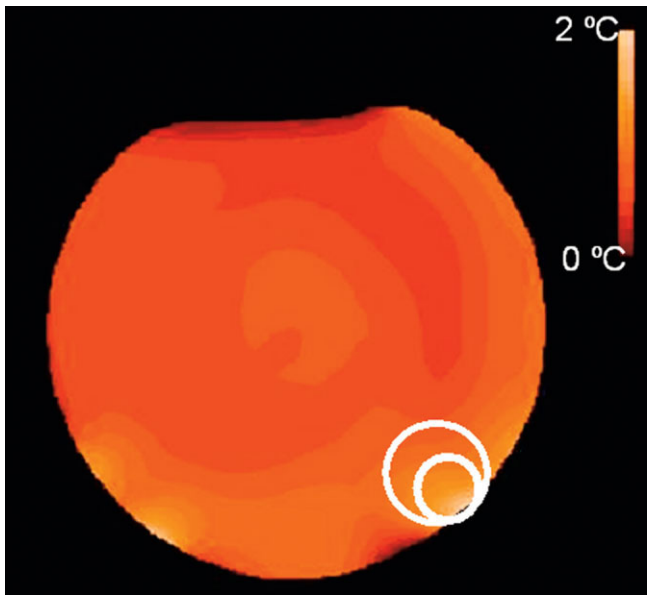

FIG. 6. Temperature map of a phantom after the application of 3 W/kg RF power for 20 min using the ^{1}H birdcage coil with the ^{13}C coil inserted. The circles indicate the regions of the maximum local SAR. The largest circle is based on IEC guidelines (10 g), and the smallest circle is based on FDA guidelines (1 g). Although the local temperature increase vs. average temperature increase is 1.8 for the 10 g location and 2.2 for the 1 g location, it remains well within safety regulations.

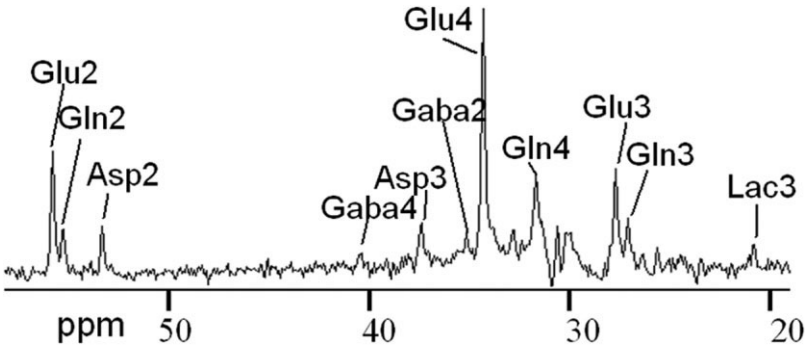

FIG. 7. Broadband ^{1}H decoupled ^{13}C MR spectrum of the human brain at 3 T under euglycemic conditions applying 30% ^{13}C-1-labeled glucose (20% w/w solution) acquired in 30 min. The resonances of the ^{13}C spins can be detected from Glu-2, Glu-3, Glu-4, Gln-2, Gln-3, Gln-4, Asp-2, Asp-3, GABA-2, GABA-4, and Lac-3.

It should be noted that the quality of the required blocking depends on the distance of the conductors to the sample. Since local ^{13}C coils normally are positioned close to the tissue, the blocking performance should be considered in terms of the maximum local B_1 disturbance rather than the amount of cross talk (in dB). We included a blocking circuit that gives a local maximum B_1 disturbance of only 11% at a distance of 8 mm from the conductor. The blocking can be improved by increasing its inductance at the expense of some intrinsic ^{13}C signal losses. However, since the initial inhomogeneity of the birdcage due to dielectric resonances is of the same order (see Fig. 4), further improvement of blocking was unnecessary.

A major advantage of a homogeneous coil for ^{1}H decoupling is that the efficiency of ^{1}H decoupling and the NOE is constant, which simplifies quantification. Although adiabatic ^{1}H decoupling could provide the same advantage, the power requirements are much higher because a threefold higher γB_1 is needed to fulfill the adiabatic condition (19), compared to the γB_1 needed for efficient WALTZ16 decoupling. WALTZ16 decouples the relevant ^{1}H spectral range of 0.9–5.4 ppm at 3 T, using a γB_1 of 350 Hz. Since the B_1 field is practically the same in the brain as in the skull, the large signals from lipids can be used to adjust the RF power for ^{1}H decoupling within a few seconds. In addition, good-quality conventional MR images can be obtained without a coil change using the current ^{1}H volume coil.

The improved efficiency of the ^{1}H field can be used to achieve CP over a large bandwidth. The sensitivity enhancement is equal to that of DEPT. However, in contrast to pulsed polarization transfer techniques like DEPT, the effect of CP does not depend on the number of protons attached to the ^{13}C nucleus, and is less sensitive to variations in J-coupling of the spins from different metabolites. From high-resolution NMR it is known that the R_4 pulse train during CP has an optimal bandwidth per unit power when the in vivo time constrains are taken into account (13). However, since this train is nominally 4/3 times longer than the WALTZ4 train, the power required to get this train inside the optimal CP duration of 1/J is $(4/3)^2$ times higher. In broadband ^{1}H-decoupled ^{13}C MRS with R_4 CP, about 50% of the SAR is caused by CP. Therefore, efficiency improvements in the new coil design regarding local SAR makes broadband CP feasible in the human head at 3T within safety guidelines.

A criterion for efficient ^{1}H-^{13}C CP is that the RF fields must be matched at both frequencies. Since our coil design combines a homogeneous field at the ^{1}H frequency with a less homogeneous field at the ^{13}C frequency, the exact matching condition may not be fulfilled in a large region of the human brain. However, at relatively low B_1 fields, RF inhomogeneities remain smaller than the typically encountered J-couplings, and therefore hardly affect the CP dynamics (21). Since such low fields are used for in vivo applications, a factor of 3.5 gain in sensitivity can still be obtained. This demonstrates that within the sensitive area of the ^{13}C coil in the human brain, efficient CP was indeed achieved.

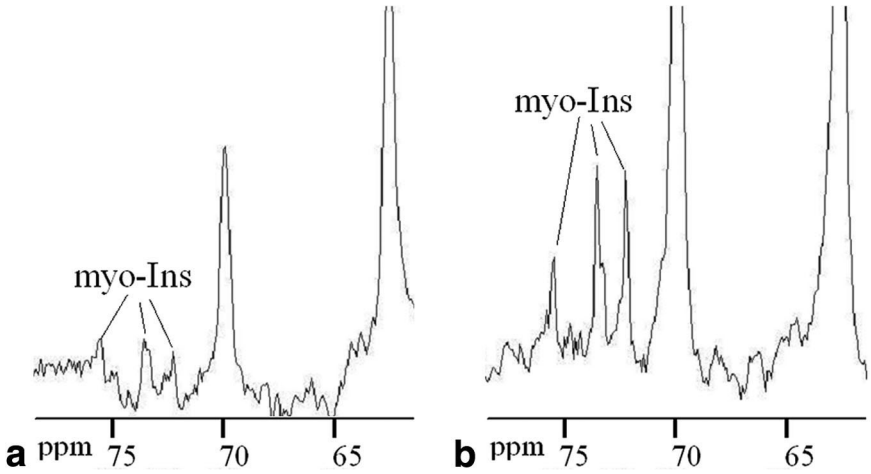

FIG. 8. Natural abundance in vivo ^{13}C MR spectra of the human brain without (**a**) and with (**b**) CP. Broadband ^{1}H decoupling was used in both measurements. The gain in SNR of ^{13}C signals of myo-inositol from the brain in the FOV of the ^{13}C coil is about 3.5.

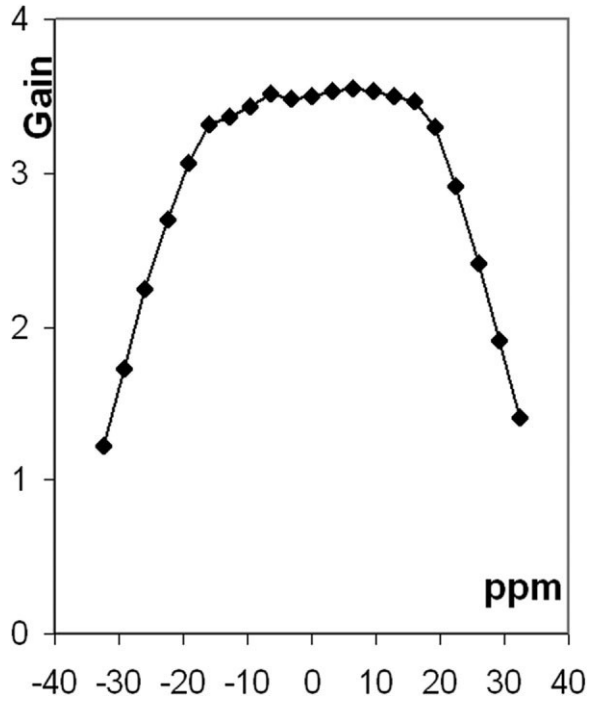

FIG. 9. Frequency profile of the gain in SNR of R_4 CP. The profile is determined using multiple off-resonance measurements acquired on a phantom with ^{13}C-1-glucose (20% w/w solution; 30% ^{13}C label), relative to an on-resonance measurement without CP.

In addition, localization techniques such as image selected in vivo spectroscopy (ISIS) (22) or outer volume suppression can be added to the CP sequence to acquire data from a selected region. The slice-selective inversion or excitation pulses can be realized with RF pulses at the ^1H channel prior to the CP section. Since the ^1H field is homogeneous, and the ^1H spins have small chemical shifts compared to the ^{13}C spins, non-adiabatic RF pulses can be used at low bandwidth, which would lead to minor extra RF heating.

Previous studies have reported the successful use of ^1H to ^{13}C polarization transfer in the human brain (23,24). However, these studies used localization techniques and were thus restricted to small regions. Since the same localization techniques can be applied in our setup, a 40% improvement in sensitivity can still be achieved (with the circularly vs. linearly polarized coil). In principle, it is always possible to optimize the performance of a coil design for one specific region of interest at the expense of versatility. Such an approach was presented by Gruetter et al. (25) using localized DEPT-enhanced ^{13}C MRS on a small region near the surface of the human brain. Our design yields excellent sensitivity by combining the quadrature ^{13}C coil (for a 1.4-fold gain compared to a linearly polarized coil) and efficient CP (a 3.5-fold enhancement compared to ^{13}C detection without NOE), which are applicable to large volumes of the human brain.

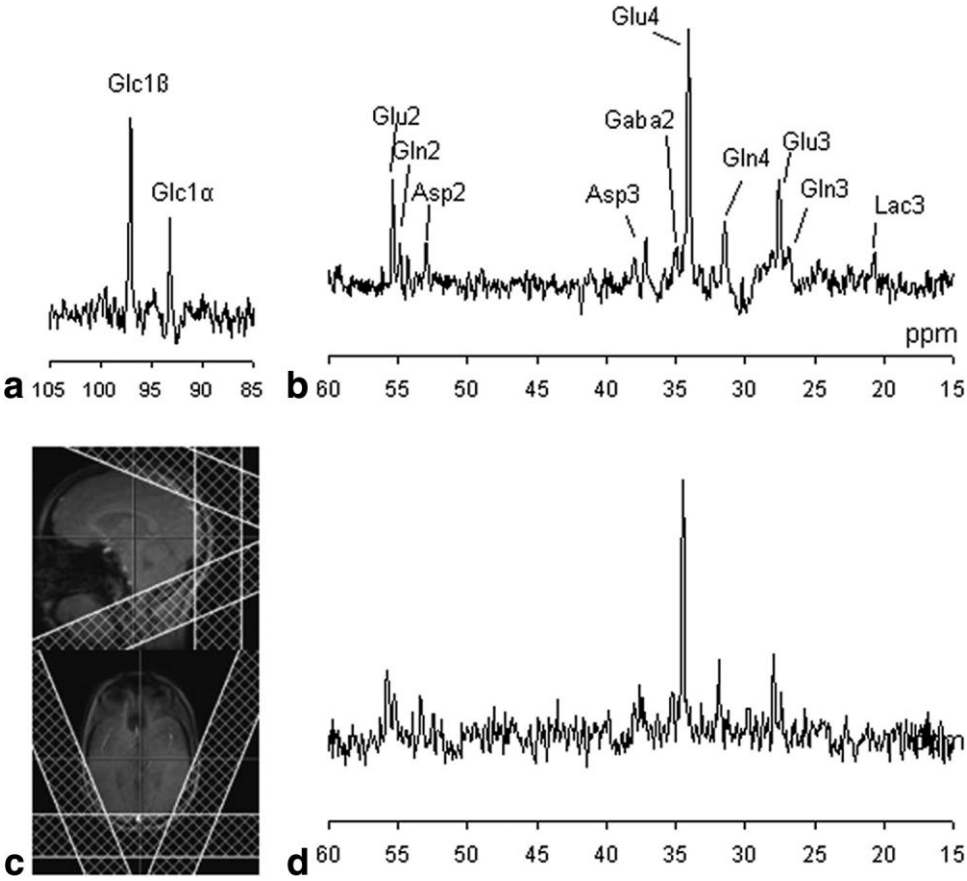

FIG. 10. ^{13}C MR spectra of the human brain (21-year-old female subject) demonstrating the effect of WALTZ4 (**a**) and R_4 (**b**) interleaved CP. CP was achieved over a larger bandwidth including glucose signals. **d:** A more than twofold SNR gain was obtained compared to a noninterleaved direct ^{13}C measurement in a 20-year-old female subject. All spectra were obtained after ^{13}C-1 labeled glucose infusion, during a 15-min euglycemic condition. The measurements were performed with outer volume suppression using broadband (10 kHz) saturation pulses (20) to suppress the lipid signals from the skull and subcutaneous fat (**c**). In addition, a ^{13}C MR spectrum of 15 min was acquired prior to the infusion for background subtraction.

CONCLUSIONS

An efficient volume head coil is introduced that can be used at 3 T for broadband ^{1}H decoupling in ^{13}C experiments within SAR guidelines. In combination with quadrature ^{13}C coils with loss-less blocking circuits, brain coverage and SNR are substantially improved compared to linearly polarized local coils. Moreover, broadband CP can be performed, which further increases sensitivity. Our coil setup allows flexibility in choosing the size and the location of the volume of interest while keeping close to the optimum polarization transfer efficiency.

The excellent sensitivity obtained was used to perform ^{13}C MR experiments on the human brain in vivo with reduced labeling percentage and at natural blood glucose levels (euglycemia). Since the substantial cost of ^{13}C-labeled compounds is one of the drawbacks that are holding up the clinical use of ^{13}C MRS, and the sensitivity of ^{13}C MRS is linearly proportional to the labeling percentage, any improvement in ^{13}C sensitivity will reduce the financial barrier that is preventing the use of ^{13}C MRS in the clinic.

ACKNOWLEDGMENTS

We thank Erik van den Bergh for helpful discussions about the ^{13}C MRS optimizations, and Ton Rovers and Rob Wolfs for realizing the coil interfaces.

REFERENCES

1. Gruetter R. In vivo ^{13}C NMR studies of compartmentalized cerebral carbohydrate metabolism. Neurochem Int 2002;41:143–154.
2. Mason GF, Gruetter R, Rothman DL, Behar KL, Shulman RG, Novotney EJ. Simultaneous determination of the rates of the TCA cycle, glucose utilization, a-ketoglutarate/glutamate exchange, and glutamine synthesis in human brain by NMR. J Cereb Blood Flow Metab 1995;15:12–25.
3. Ross B, Lin A, Harris K, Bhattacharya P, Schweinsburg B. Clinical experience with ^{13}C MRS in vivo. NMR Biomed 2003;16:358–369.
4. Center for Devices and Radiologic Health. Guidance for the submission of premarket notifications for magnetic resonance diagnostic devices. Rockville: Food and Drug Administration; 1998. p 21.
5. International Electrotechnical Commission. International standard, medical equipment—part 2: particular requirements for the safety of magnetic resonance equipment for medical diagnosis. 2nd revised ed. Geneva: International Electrotechnical Commission 601-2-33; 2002. p 29–31.
6. Adriany G, Gruetter R. A half volume coil for efficient proton decoupling in humans at 4 Tesla. J Magn Reson 1997;125:178–184.
7. Collins CM, Liu W, Wang J, Gruetter R, Vaughan JT, Ugerbil K, Smith MB. Temperature and SAR calculations for a human head within volume and surface coils at 64 and 300 MHz. J Magn Reson Imaging 2004;19:650–656.
8. Fitzsimmons JR, Brooker HR, Beck B. A comparison of double-tuned surface coils. Magn Reson Med 1989;10:302–309.
9. Doddrell DM, Pegg DT, Bendall MR. Distortionless enhancement of NMR signals by polarization transfer. J Magn Reson 1982;48:323–327.
10. Hartmann SR, Hahn EL. Nuclear double resonance in the rotating frame. Phys Rev 1962;128:2042–2053.
11. Artemov D, Bhujwalla ZM, Glickson JD. In vivo selective measurement of {1-^{13}C}-glucose metabolism in tumors by heteronuclear cross polarization. Magn Reson Med 1995;33:151–155.
12. van den Bergh AJ, van den Boogert HJ, Heerschap A. Heteronuclear cross polarization for enhanced sensitivity of in vivo ^{13}C MR spectroscopy on a 1.5T MR system. J Magn Reson 1998;135:93–98.
13. Luy B, Glaser SJ. Broadband heteronuclear Hartman-Hahn sequences with short cycle times. J Magn Reson 2000;142:369–371.
14. Seifert F, Rinneberg H. Adaptive coil control: SNR optimization of a TR volume coil for single voxel MRS at 3T. In: Proceedings of the 10th Annual Meeting of ISMRM, Honolulu, Hawaii, USA, 2002. p 162.
15. Johnson G, Jung KJ, Wu EX, Hilal SK. Self-correction of proton spectroscopic images for gradient eddy current distortions and static field inhomogeneities. Magn Reson Med 1993;30:255–261.
16. Cline H, Mallozzi R, Li Z, McKinnon G, Barber W. Radiofrequency power deposition utilizing thermal imaging. Magn Reson Med 2004; 51:1129–1137.
17. DeFronzo RA, Tobin JD, Andres R. Glucose clamp technique: a method for quantifying insulin secretion and resistance. Am J Physiol 1979; 237:E214–E223.
18. Witjes H, Melssen WJ, in't Zandt HJ, van der Graaf M, Heerschap A, Buydens LM. Automatic correction for phase shifts, frequency shifts, and lineshape distortions across a series of single resonance lines in large spectral data sets. J Magn Reson 2000;144:35–44.
19. de Graaf RA, van Eijsdeb P, Brown P, McIntyre S, Nixon T. Evaluation of broadband decoupling schemes for in vivo NMR spectroscopy. In: Proceedings of the 12th Annual Meeting of ISMRM, Kyoto, Japan, 2004. p 191.
20. Choi IY, Tkac I, Gruetter R. Single-shot, three-dimensional "non-echo" localization method for in vivo NMR spectroscopy. Magn Reson Med 2000;44:387–394.
21. Chiarparin E, Pelupessy P, Bodenhausen G. Selective cross-polarization in solid state NMR. Mol Physics 1998;95:759–767.
22. Ordidge RJ, Connely A, Lohman JAB. Image-selected in vivo spectroscopy (ISIS): a new technique for spatially selective NMR spectroscopy. J Magn Reson 1986;66:283–294.
23. Shen J, Petersen KF, Behar KL, Brown P, Nixon TW, Mason GF, Petroff OAC, Shulman GI, Shulman RG, Rothman DL. Determination of the rate of the glutamate glutamine cycle in the human brain by in vivo C-13 NMR. Proc Natl Acad Sci USA 1999;96:8235–8240.
24. Gruetter R, Adriany G, Merkle H, Andersen PM. Broadband decoupled, H-1-localized C-13 MRS of the human brain at 4 Tesla. Magn Reson Med 1996;36:659–664.
25. Gruetter R, Seaquist ER, Ugerbil K. A mathematical model of compartmentalized neurotransmitter metabolism in the human brain. Am J Physiol Endocrinol Metab 2001;281:E100–E112.